GBT Memo 326

The GBT Extended Shutdown 2025: Recommissioning Report

Larry Morgan, Ryan Lynch, Emily Moravec, Pete Chestnut, Simon Dicker, David Frayer, Jay Frothingham, Brenne Gregory, Matthew Harrison, Bryan Jenkins, Walter Klahold, Paul Marganian, Anthony Minter, Brandon Moore, Karen O'Neil, Kathlyn Purcell, Jason Ray, Charles Romero, Pedro Salas, Anika Schmiedeke, Evan Smith, Sheldon Wasik, Thomas Chamberlin, Nathaniel Sizemore & William Wallace

June 29th, 2026

Abstract

The Green Bank Telescope underwent an extended shutdown from May to September 2025 to support upper feedarm repainting, foundation and track work, wheel replacement, and annual maintenance activities. Because the paint removal posed contamination risks to receiver cabin instrumentation, nearly all of this equipment was removed and power to the receiver cabin disconnected for the duration of the shutdown. This constituted the longest loss of cabin power since telescope commissioning and so extensive preparation, benchmarking observations, and coordinated recommissioning activities were undertaken to minimize operational disruption and verify post-shutdown system performance.

Here we summarize the recommissioning of the telescope control, IF/LO, receiver and backend systems following reinstallation. Operational checks demonstrated successful restoration of telescope systems, with a reestablishment of nominal performance metrics.

Noteworthy results from these efforts include significant engineering work on the L- and X-band receivers, for which updated calibration measurements were made. Several persistent or newly identified issues were characterized during recommissioning, including satellite-related RFI at X- and K-band frequencies, polarization-dependent RFI contamination at X-band, elevated KFPA noise associated with new Kuiper downlinks, and gain differences between X-band wideband and narrowband observing modes.

MUSTANG-2 recommissioning demonstrated nominal detector and OOF performance, while dedicated tests showed that the newly installed feed defroster does not introduce measurable degradation to MUSTANG-2 observations and may remain operational during science use.

Overall, the telescope and associated instrumentation were successfully returned to operational status following the shutdown, with only minor residual issues and calibration tasks remaining.

1 Summary

The majority of equipment stored in the receiver cabin on the feedarm of the GBT was removed from the telescope during an extended shutdown period from early May to late

September 2025.

An extended shutdown period was necessary in order to address the need for paint removal and reapplication on the GBT upper feedarm. Further, track and foundation work were required, along with ongoing efforts to carry out wheel replacements. This is in addition to the regular summer maintenance necessary for operation of the GBT - inspection of motors, blowers, gearboxes, brakes, etc. as well as elevator and access concerns. A summary timeline of the primary maintenance, painting, foundation, etc activities is shown in Fig. 1.

Work was carried out in order to prepare for this unprecedented event. This included several phases of preparation, followed by recommissioning activities -

- Consultation with senior members of staff in order to determine potential improvements or essential maintenance and the prioritization of those projects.
- The formation of a shutdown 'Tiger Team' tasked with preparing for the shutdown and anticipating necessary duties/assignments to ensure the smoothest possible transitions into and out of shutdown.
- Benchmarking of instruments. Particularly for the cases of instruments that were to undergo significant repair and/or upgrades through the shutdown, a program of benchmarking observations was undertaken in order to form a basis for comparison when those instruments were reinstalled. The primary goal of this task was to provide a 'clean slate' for comparison so that any indications of equipment failure or error following the shutdown could more easily be traced to its cause.
- Recommissioning of individual systems.

2 Individual Systems

2.1 TelOps / Electronics / SDD Startup Tasks

This report is largely directed at the signal path electronics most commonly encountered in scientific operations, the receivers, IF system, etc. However, there are many other systems inherent in the general operation of the GBT which are necessary to overall operations. These were also subject to recommissioning checks and the most relevant of these are recorded below.

2.2 PTCS

The Precision Telescope Control System (PTCS) is a name for a suite of metrology systems, servos and control software which deliver the pointing, collimation and surface accuracy required to operate the GBT at high ($\gtrsim$ 40 GHz) frequencies. These necessitate a separate dedicated effort of their own for recommissioning efforts and are thus outlined here. The specific systems which were defined as requiring validated performance are listed in Table 2, along with a short summary of the testing outcomes.
Note that holography Measurements are part of the regular (spring and fall) PTCS activities.

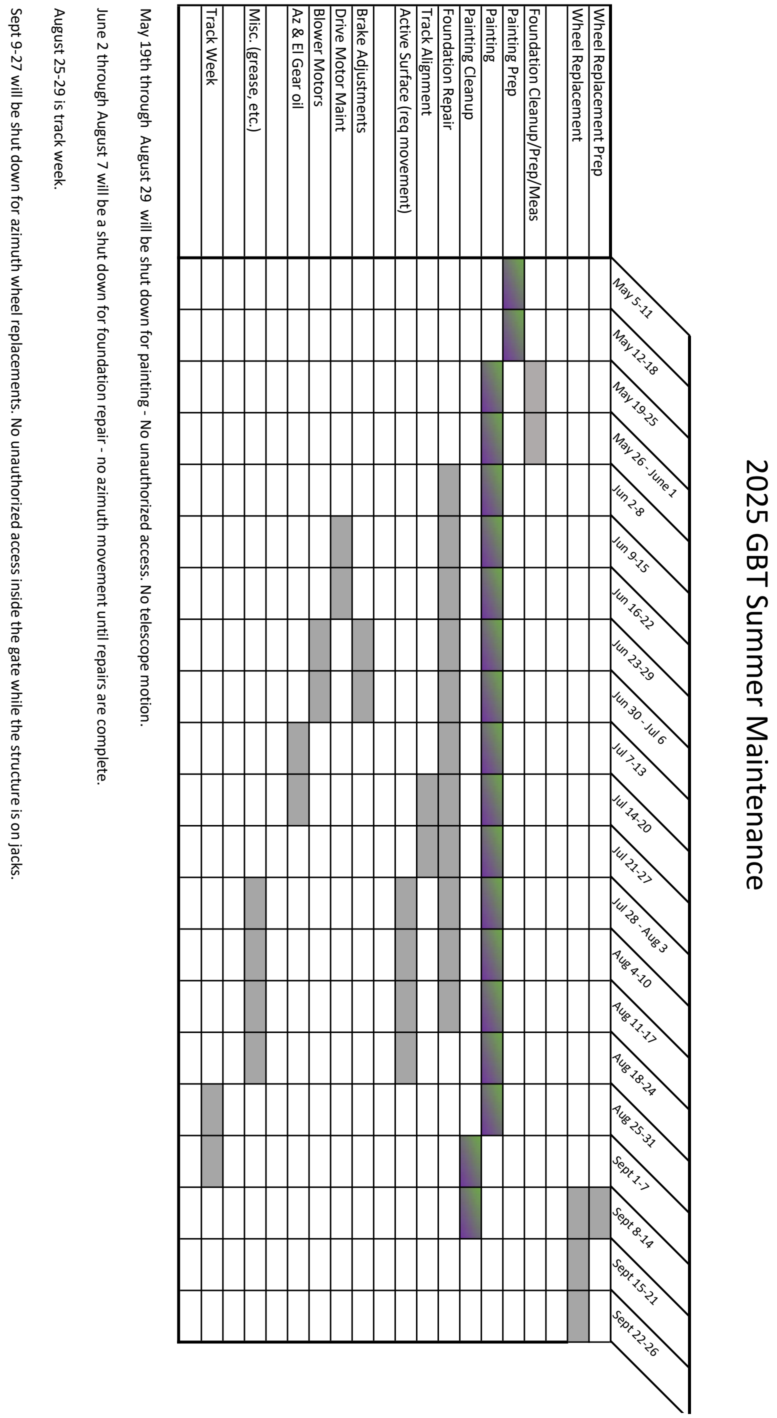

Figure 1: 2025 Summer Maintenance Schedule

Item	Notes
• Inspect Cabling for obvious damage • Inspect Turret gasket and clean as necessary • Test PF Boom, sterling mount, subreflector and turret for motion • Receiver room floor tiles removed and floor painted • Test Azimuth and Elevation Movement • Ensure HVAC system is free of debris and return to service • Inspect PF boom ball screw and subreflector actuators • Turn on Motor Rack • Turn on PF rack	signed off by **B.Jenkins**
• Temperature Sensors	Sensor gbtts1_2001 removed during shutdown and subsequently reinstalled. Two other air temperature sensors (gbtts1_2003 and gbtts1_2006) were removed but not reinstalled because they aren't used anymore. **J.Ray**
• Feed Defroster	A new feed defroster was designed and built during the summer by M.O'Ganian. This was slightly larger than the previous defroster and so the ARGUS vane mount was rotated by 180°. Further, a higher capacity soft starter was required for remote operation. Science checks indicate that the new feed defroster may be left on during MUSTANG observations, which was not true of the previous defroster.**J.Ray**. Please see also 2.4.6
• Quadrant Detector	Quadrant detector was removed for the shutdown period. Reinstallation required several 'tunings'. Follow-up checks/calibration were performed by P.Salas. **J.Ray**

Table 1: Summary of TelOps/Electronics/SDD Startup Tasks

System	Related Project ID	Notes
Dynamic Corrections Active Surface Focus Tracking Model Pointing Model (6b) SCU/CCU Antenna FEM model Gravity Zernikes Weather Stations Temperature Sensors Quadrant Detector	TGBT25B_603_10 D. Frayer 2025.09.02	Operational checks were carried out and confirmation was made that collected data were valid via CLEO output, FITS keyword checks or by the success of regular observations.
Track Lambdas Inclinometer Data	TPTCSPNT_250823 D. Frayer 2025.08.23	Operational checks were carried out. Valid data were seen and confirmed with PTCS measurements of the track and holography map measurements.
Subreflector		Subreflector basic motions have been checked out via regular observing/focus tracking. SubBeamNod still needs to be validated as of 2025.09.29.
OOF Zernikes	TRCO_251002_Ka	Valid data verified with Ka+CCB.
Holography Receiver	TPTCSHOL_250919 P. Salas 2025.09.19	Operational checks were carried out and valid data were confirmed with PTCS holography map measurements

Table 2: Summary of PTCS Recommissioning Checks

The task will not be tracked as a 'startup' activity and so results are not reported here.
A further note is made here that full quadrant detector recalibration was intended but not completed. Full checks of the illumination of the detector was completed down to ∼7 degrees elevation (*P.Salas, priv. comm.*) but the offsets have not been checked as of May 2026.

2.3 I.F. Rack/L.O. System

The I.F. rack was not removed from the telescope during the shutdown period, although the L.O. system was. As nearly all scientific observations make use of these systems, these were the first to be re-commissioned/tested following the shutdown. Tests were performed under the projects TSCI_KAREN_19 and TSCI_KAREN_20 on the 26th of August, 2025. Eight VEGAS banks were set up to collect data, using four optical drivers. By flipping the optical driver selections, it was possible to ensure that data were being recorded (via the L-band receiver). Checks were made via CLEO readouts to ensure that the I.F. rack and converter rack were communicating. Similarly, switching optical drivers and changing the filter width indicated changes to the signal power in line with expectations (e.g. increasing the filter width by a factor of three led to a change in signal power of 5 dB).

The L.O. system was checked by changing the L.O. frequency and observing changes using GBTIDL. Milky Way HI emission was observed, in addition to expected RFI at 1381 MHz.

2.4 Receivers

At the start of the shutdown period the following receivers were installed on the telescope - PF800, L, C, X, KFPA, Q, Argus, Holography and MUSTANG2. PF800 was brought down and UWBR installed on 5th of May to allow for UWBR commissioning tests. The L, C, X, KFPA, Q, Argus and MUSTANG2 receivers were brought down over the period from the 6th to 9th of May. UWBR was removed on the 12th, the holography receiver was brought down on the 15th and the holography horn was removed on the 20th.

It should be noted that the L- and X-band receivers were anticipated to be refurbished during the shutdown period and so special attention was paid to their performance (the KFPA was also originally expected to have some electronic work performed over the shutdown but this did not take place).

During the Summer of 2025 an extensive three-year summer maintenance campaign for Argus was successfully concluded. A detailed breakdown of the work executed falls outside the scope of this GBT memo. (Details on the extent of the work can be provided by the instrument friend[1] upon request).

Following the shutdown, the L- and S-band receivers were installed on the 25th of August, followed by PF800 on the 26th. It was the intention to have these receivers installed as soon as possible (following the reinstallation of the LO system) in order to take advantage of the track work period for testing of the IF path, etc. Both the S-band and the PF800 receivers were installed in addition to the L-band receiver so that, if any issue were seen with the L-band receiver, a comparison could be made to rule out any issues arising from the refurbishment work done over the summer on the L-band receiver.

Short notes on the checkout of each receiver following re-installation are recorded here.

2.4.1 L-Band

An initial checkout was performed on the 25th of August under TGBT25B_603_01 by E.Smith. As the subreflector was found to be inoperable and stuck in a limit for these observations, they were useful as a test of the full signal path but have otherwise been disregarded. The subreflector issue was resolved and subsequent checkouts were performed as outlined in Table 3.

In addition to tests of the L-Band receiver performance, we wanted to measure a new set of Tcals in order to account for the internal maintenance of the receiver, as well as the heavy

[1]A.Schmiedeke at the time of writing

Session	Date	Notes
TGBT25B_603_01	Aug 25, 2025	Preliminary checkout. Inoperable subreflector but test of full signal path
TGBT25B_603_04	Aug 27, 2025	Full antenna motion checkout. Observed 3C295
TGBT25B_603_06	Aug 29, 2025	Noise tests, staring at North Celestial pole
TGBT25B_603_08	Aug 30, 2025	First set of low-flux Tcal measurements
TGBT25B_603_18	Sep 20, 2025	Second set of low-flux Tcal measurements
TGBT25B_603_20	Oct 9, 2025	Third set of low-flux Tcal measurements

Table 3: Summary of L-Band Recommissioning Checks

broadband RFI from temporary traffic lights located at Riley Run bridge, north of the GBT and centred around 900 MHz. For these reasons, the Mueller matrix for the L-band receiver will also have to be done. It was not in scope for this recommissioning; the first GBT project that requires precise polarization calibration will have to measure it.

In order to measure Tcals adequately, a series of low-flux quasars on the order of 1-2 Jy were used. This was done because:

- The typical "gold-standard" sources used in other receiver checkouts (e.g. 3C295) are so bright that it is impossible to hold a balanced IF system between the ON and OFF positions. The difference between them at the last power sampler (VEGAS inputs) can vary by more than 7 dBm, which cannot be contained by the recommended range of -18 to -22.

- Tcals are measured using an assumption of the known flux of the quasars observed. These quasars were taken from the VLA calibrator catalog [2,3], and had varying degrees of recency in their measurements. To avoid relying on a single quasar with an out-of-date flux measurement, we used a series of quasars and averaged 3-4 different measurements that returned similar results.

Tcals were derived using /home/astro-util/TRCO/tcal_calc_Lband.pro. This is a variation of the standard gbtidl script for determining Tcals, but was created to contain the known flux polynomial coefficients in the getFluxCalib function.

Tcal measurements were divided into 5 separate IF windows. The window size was 187.5 MHz, with 32768 channels and a 10% overlap, leading to center frequencies of 1143.75, 1312.5, 1481.25, 1650, and 1818.75 MHz. This was to protect parts of the band from unbalancing due to heavy RFI from GPS, Iridium, and CARSR Radar. Furthermore, the 'filter out' observations were not used - due to the same recommendation for science observations, the traffic light RFI caused balancing issues for frequencies above 1.3 GHz, as seen in Fig.2, where the 'clean' part of the spectrum is significantly different between the filter in and filter out data.

Tcals were determined by combining the individual IF measurements along the spectral axis, smoothing by a certain factor, and using the *numpy polyfit* routine to fit a smoother

[2] `https://science.nrao.edu/facilities/vla/observing/callist`

[3] `https://www.vla.nrao.edu/astro/calib/vlacal/cal_mon/last/`

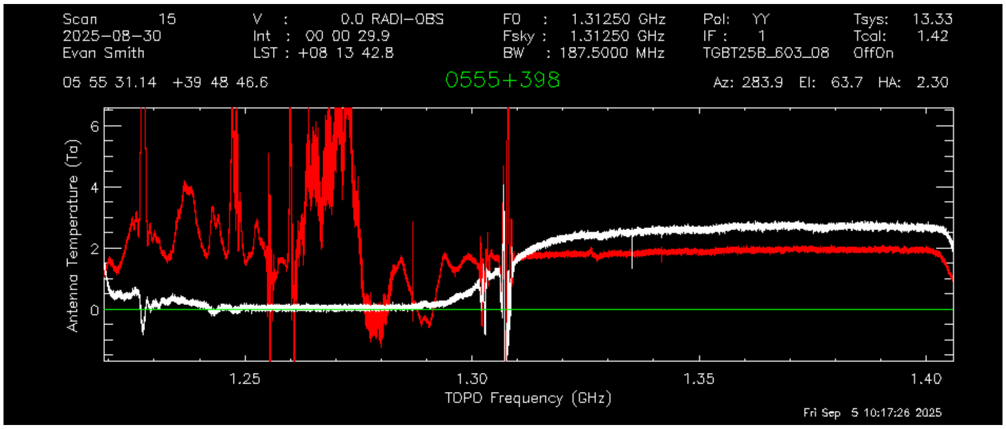

Figure 2: 'getps'-reduced spectrum showing the effects of RFI arising from a local temporary traffic light.

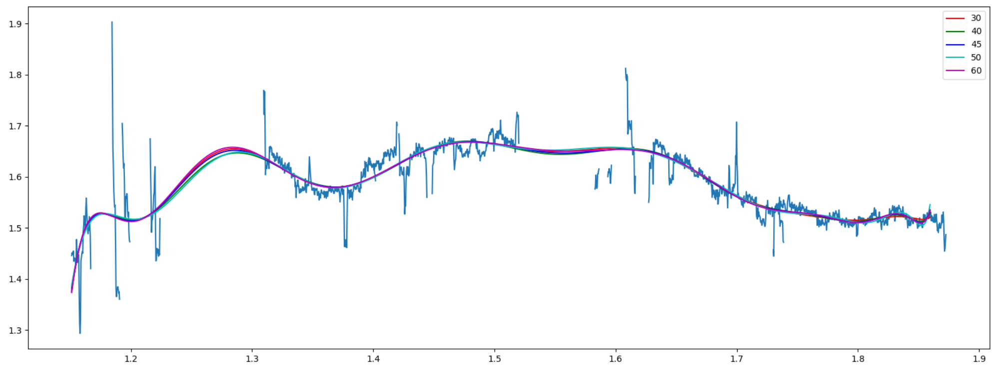

Figure 3: L-Band TCal determination for data taken during the TGBT25B_603_08 session.

curve. The smoothing factor and fit order were chosen on a case-by-case basis for each diode. An example of the low X diode is shown in Fig.3, with several fit orders shown. This is with a smoothing factor of 64.

Polarization Comparison/Noise Measurements

A comparison between the L-band polarizations was performed by K.O'Neil. The result is that the noise levels for L-band XX and L-band YY appear to be the same - see Fig.4. The dataset comprises all frequency-switched observations obtained toward the celestial pole during project TGBT25B_603_06 on 2025 August 28, with the data subsequently reduced using frequency-switch processing. As a consequence of the reduction process, the full-bandpass images exhibit the characteristic negative aliases and discontinuities associated with frequency switching, including inverted copies of both the Galactic emission and the noise structure.

For the data that had a baseline applied, the same regions and power were used to fit the polynomial for each polarization, to allow for easy comparison (but not the same polynomial).

Figure 5 shows the difference between measured and predicted RMS noise in the XX

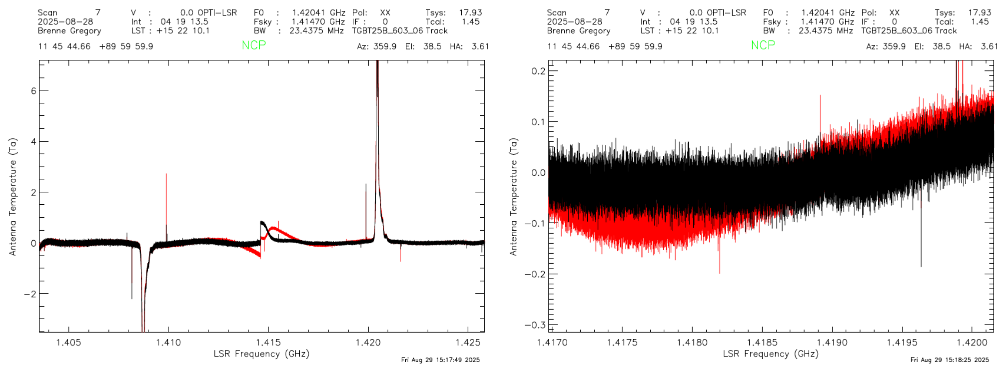

Figure 4: Spectra used for noise determinations for the L-Band receiver. Left - full bandpass of baselined spectra, XX polarisation is in red with YY in black. Right - expanded view of spectrum shown on the left

(black) and YY (red) polarizations for these observations accumulated over a period of roughly 12 hours. The dashed lines show this difference as a fraction of the predicted RMS noise. It can be seen that noise is higher in the YY polarization than for the XX. However, both polarizations exhibit at least superficial stability over a cumulative exposure period of ∼4.3 hours and are continuing to integrate down.

2.4.2 C-Band

'Receiver baseline test' observations were performed on April 23rd, 2025 by Jay Frothingham under project code TGBT25A_608_04. The receiver was removed from turret slot N5 (179 deg) on May 6th, 2025. No physical changes were made to the receiver during the shutdown period.

The receiver was reinstalled in turret slot N3 (259 deg) and re-commissioning observations were performed on September 2nd, 2025 by Jay Frothingham under project code TGBT25B_603_10. A regular receiver checkout was subsequently performed on September 27th, 2025 by Ryan Lynch under project code TRCO_250927_C.

Results/Conclusions

The behavior of the C-band receiver has not changed after the summer 2025 extended maintenance shutdown. A few recurring issues should be monitored, but none were found to be 1) new or 2) operationally impactful. In most cases, restarting managers and/or resubmitting scripts is sufficient to continue observing.

2.4.3 X-Band

X-Band tests were carried out by L.Morgan on the 20th of September, 2025. These were 'recommissioning' exercises exceeding normal 'checkout' procedures due to engineering work carried out over the shutdown period. Data were taken under TGBT25B_603_19.

No major issues were found and the X-band receiver is ready for scheduled observing, though it should be noted that the database TCal values were not updated due to poor

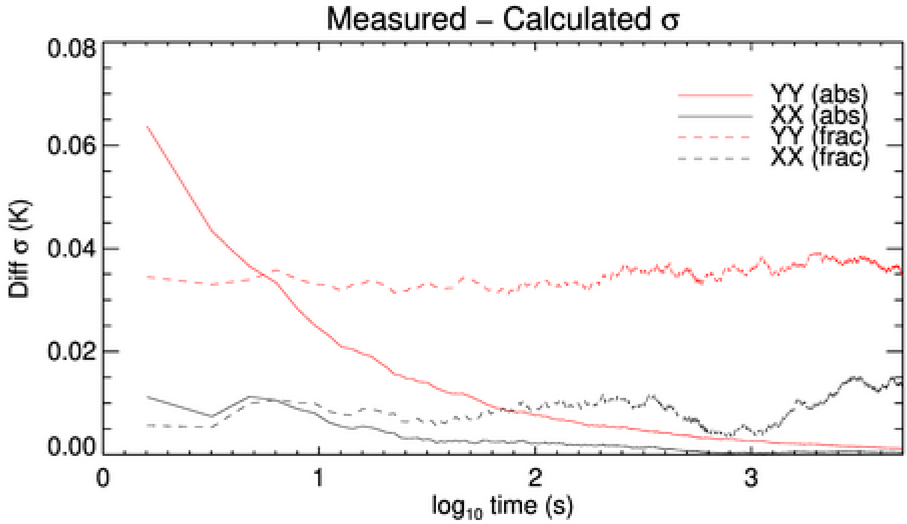

Figure 5: The difference between measured and predicted RMS noise in the XX (black) and YY (red) polarizations. The dashed lines show this difference as a fraction of the predicted RMS noise.

weather during these observations. **N.B. TCal measurements were made on the 9th of October, 2025 under the project/session code TGBT25B_603_21, with a subsequent update of the TCal database.**

A note is here made of differences in the gain measurements of the X-band receiver depending on whether the signal path uses the wideband or narrowband route. Whether this is due to actual instrumentational gain differences, or due to filtering of external radiative contributions in the narrowband mode has not been determined. In any case, it is noted that the 'system' TCal values recorded in the database (and therefore used by default when reducing data) as well as the GBT sensitivity calculator are appropriate to the wideband mode. Any observations performed in narrowband mode should make appropriate calibration measurements if necessary.

It is also noted here that a large SNR deficit reported in some JPL Voyager observations (AGBT25A_997_03) could not be reproduced with these observations. The specific IF routing used by JPL may introduce a small sensitivity loss, but only at the level of a few tenths of a dB, not the >5 dB discrepancy previously observed. The Voyager signal strength, system noise, and pointing/ephemeris all appeared nominal.

2.4.4 KFPA

KFPA tests were carried out by L.Morgan on the 3rd of September, 2025. These were largely regular checkout procedures - no engineering work was carried out on this receiver over the shutdown period. Data were taken under TGBT25B_603_11.

Weather conditions were marginal but acceptable for K-band - Patchy cloud, with a zenith tau value of ∼0.16 at 22 GHz.

Unedited notes from the checkout session are presented in Appendix A. A summary is as follows,

- Initial peak and focus scans showed baseline ripple, which improved after refocusing. More generally, ripple was present in the APFs throughout the observations and was consistently stronger for beams 3/7 than for 4/6, in agreement with previous KFPA results.

- Observations also showed substantially more RFI than expected. In particular, strong and apparently new interference was consistently present near 19.6 GHz and across 20.5–20.65 GHz, likely associated with Kuiper satellite downlinks.

- Measured RMS noise levels were approximately 7% above theoretical expectations, potentially as a consequence of the observed RFI environment. System temperatures ranged from 62–180 K and were noticeably elevated for beams 5–7, broadly consistent with pre-shutdown performance and likely related in part to less accurate TCal values for those beams.

- KFPA broadband mode was not explicitly tested during this observing session due to lack of time, but subsequent tests on 9 September (TGBT25B_603_12) indicated stable and nominal broadband performance for beams 1 and 2.

2.4.5 Ka/CCB

The Ka-Band receiver and CCB backend were not subject to any engineering work during the 2025 extended shutdown. Because of this, no particular recommissioning efforts were planned to return them to operations. However, upon the reinstallation of the receiver, it was found that the calibration control board was not receiving the correct voltage levels due to failing chips in the MCB. This led to a failure of external control of the noise amplifiers.

The MCB was repaired and, later, a further software/sampling issue was identified.

> It was discovered that the `MCBServer` process on host `fire` (using USB–serial links) was operating more than an order of magnitude slower than the corresponding process on `wind` (using native serial interfaces without USB conversion).
> For devices using the `ftdi_sio` driver, the default latency timer is 16 ms. By adding `ATTR{latency_timer}="1"` to the `10-nrao-monctrl.rules` configuration, the latency was reduced from 16 ms to 1 ms. This change significantly improved the performance of the USB adapters and eliminated the delays that were causing failures in Ka-band operations.

Priv. Comm. Matthew Harrison

2.4.6 MUSTANG2

Tests were carried out by S. Dicker and E. Moravec on the 10th of October, 2025. Data were taken under TGBT25B_607_01. A complete write-up of the receiver checkout and testing can be found at https://nrao.atlassian.net/wiki/x/BwA1Ew. A summary follows:

MUSTANG-2 was recommissioned following reinstallation on the telescope, including cryogenic cooldown, readout verification, detector noise characterization, OOF validation, and a series of dedicated blower-vibration tests. On-sky checkout observations confirmed that the OOF system operated correctly with quadrant-detector corrections disabled, detector performance was nominal, and the instrument was ready for science scheduling. Additional daytime monitoring showed that beam quality degraded within $\sim$15 minutes after an OOF correction, providing a useful operational constraint.

Further notes regarding MUSTANG2 tests of potential impacts of the GBT turrets feed defroster (‘blower’) may be found in Appendix B.

References

DePree, C., Armentrout, W., Beasley, T., et al. 2023, NRAO RFI Memo Series #154

Morgan, L., Klahold, W., Harrison, M., & Paul, M. 2024, GBT Memo Series #314

Appendix A:

Notes from Observing Sessions

Individual Checkout Sessions

L-Band

TGBT25B_603_01: We just aimed for a full basic checkout with the goal of testing the full IF/LO system from receiver to backend. The subreflector had issues - something had hit a delta limit and we could not use the subreflector. We pressed on with the inefficiency and indeed found low gain, but nothing more could be gained from this session.

There was some RFI detected during this session that Karen and Toney investigated as part of the IF/LO checkouts.

TGBT25B_603_04: This is another attempt at a normal L-Band checkout, this time with full antenna and subreflector motion. Everything looked nominal during this session. See details in [gbtinfo] email dated 08/27/2025, copied below:

> I did the L-band checkout this afternoon. Before I took control, we saw a 'Y2 TACH VS ENCODER FAULT' fault come up, and testing by Bryan, Kasey, and Paul assured that it would not affect observations - focus scans ran fine. Other than that, the data all looks really good tonight before I dive more into it tomorrow. I did the following:
>
> - TCal measurements on 3C295 and 3C286
> - Pulsar scans of B1133+16 and B1937+21
> - Extragalactic HI scans of M82, UGC 8091, and UGC 9965
> - RFI scan from Az 190 to 360
> - 2 MHz RFI check. I don't think I see the RFI, but I am not sure if I had the right configuration or if I was looking for the right thing.

TGBT25B_603_06: These were noise tests, done in the same manner as the other receivers. We stare at the North celestial pole as that is the one spot in the sky that does not change in background sky radiation or in AzEl coordinates. We took an extra precaution of stepping the LFC 2mm periodically to avoid a standing wave/harmonic. This was advised by Toney M.

TGBT25B_603_08: This was the first set of low-flux Tcal measurements, with targets picked following the description above. We picked 0555+398, 0632+103, and 0738+177 in this first session. We found that there were discrepancies between the sources and Tcals couldn't be resolved with just this dataset. An example for the Low R diode is shown in Fig.6.

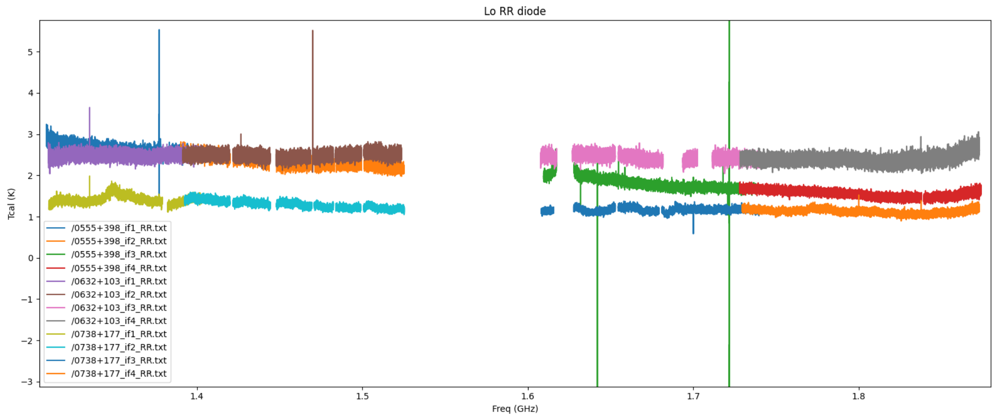

Figure 6: Multi-Source L-Band TCal determinations for data taken during the TGBT25B_603_08 session.

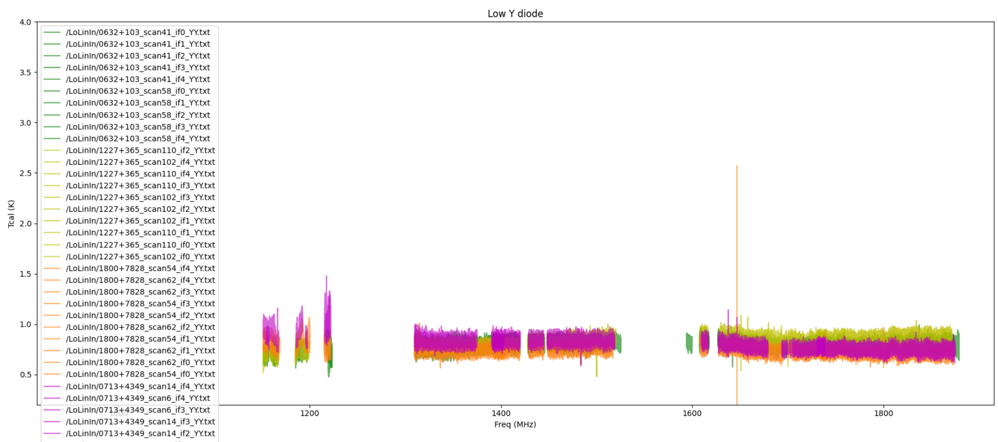

Figure 7: Multi-Source L-Band TCal determinations for data taken during the TGBT25B_603_18 session.

TGBT25B_603_18: This was the second attempt at low-flux Tcal measurements. I observed the following sources (see Fig.7:

0217+7349	0713+4349	1153+8058	1227+365	1347+122
1400+621	1407+284	1419+5423	1800+7828	2355+4950

After running through Tcal checks, I decided to average 3 sources together for the final product: 0632+103, 1227+365, and 1800+7828. There was very little usable data in the first IF window due to the traffic light RFI (among lots of other sources). However, a few spots could be picked as relatively clean, and this served to 'anchor' the Tcal determination below 1300 MHz.

TGBT25B_603_20: During the maintenance period on Oct 1, 2025 it was discovered that the L-band radome was torn slightly. From Walter K, It was noticed this morning that there is a small, ∼1 cm length tear at the edge of the L-band radome. It is unknown how or when this developed, but there is a possibility that there is water inside the feed at the moment. The current plan is to replace the radome during this Friday's maintenance, but in the meantime the tear has been temporarily mended with sealant.

We reran a quick check of the low-flux Tcals to make sure they were still matching up to the recent measurements in session 18. I just observed 0217+7349 and 1800+7828 and only the low noise diodes, and while there was a slight difference, it was not enough to warrant a full redetermination.

C-Band

Full notes on the C-Band recommissioning observations may be found at https://nrao.atlassian.net/wiki/x/
Relevant excerpts from that source are:
Issues to monitor:

- Active surface failure to power up, requiring additional restarts by the Operator
  noted as an issue to monitor
- Y2 tach encoder fault
  resolved after a restart of the SCU
- VEGAS banks dying during scans
  resolved via manager restart

Email Report from J.Frothingham

C-band checkout was mostly uneventful. I checked a test tone, did position and frequency switching on OH masers, and ran high and low tcal scripts on 3C295 and 3C286. I believe RFI scans will be run later in the night.
Data can be found under TGBT25B_603_10.
I'll go through the data more thoroughly over the next few days, but I didn't see anything immediately concerning or drastically different from previous checkouts.
The active surface required some additional rebooting from Dave - it initially came up with 50% of the actuators disabled. After restarting a second time, it came back with 54 actuators disabled. This had increased to about 75-80 actuators disabled by the end of my time.

X-Band

Observing notes from L.Morgan on the 20th of September, 2025 - Data were taken under TGBT25B_603_19.

I saw multiple issues with peak/focus scans, none of which prevented me getting good pointing corrections but still worth making note of. Many of the peak/focus scans from my session had significant gradients over the scan. This was worse for some scans than others but present in almost all scans. The 'worst' of these was the first (Fig.8), on 3C287 (near 3C286, I don't know why APF chose 3C287 over 3C286, they are both 'gold standard' sources in the xband pointing catalogue). I immediately repeated the APF on this source, with similar

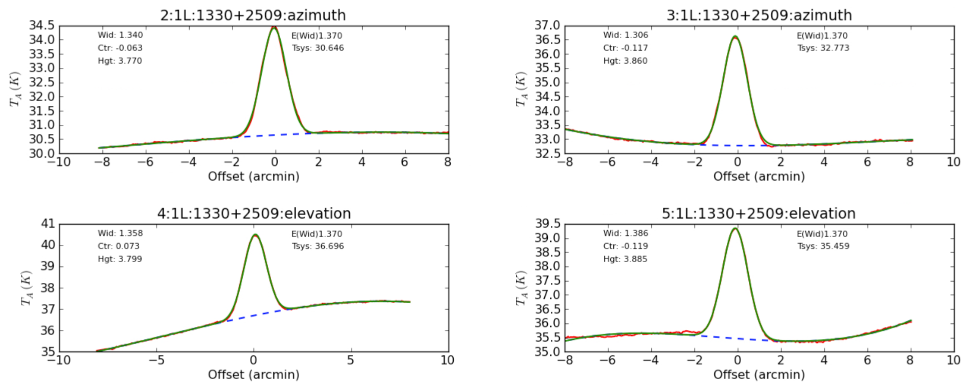

Figure 8: X-Band peak scans on 3C287 (1330+2509)

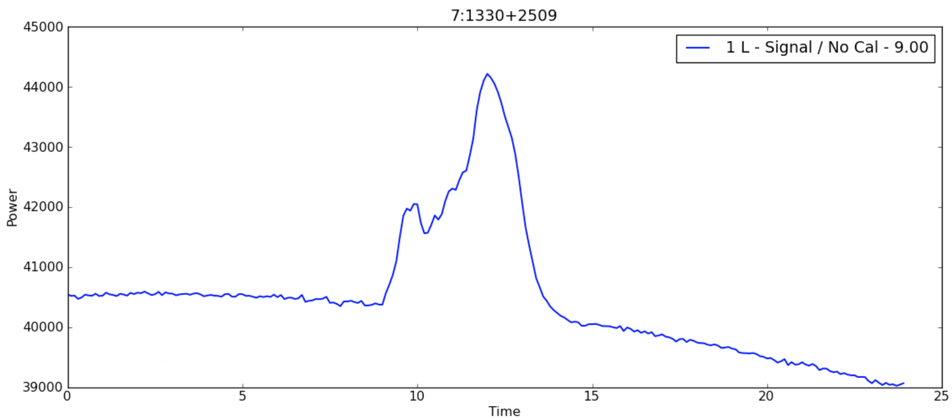

Figure 9: Single azimuthal X-Band peak scan on 3C287 (1330+2509)

results. However, the first scan of that APF showed some potential RFI or other issue (Fig. 9). The next set of APF scans were mostly unremarkable but the set following that showed several spikes which I'm unable to account for (Fig. 10). A possible explanation for all of these issues would be if RFI were impacting the obs. This would explain the spikes and potentially the gradients too.

I observed the standard receiver checkout script, which includes flux cal measurements on 3C286 and a test tone observation. Scans 13/14 (Fig.11 - top) are an OffOn pair (note that scan 12 failed to balance and was aborted). Average Ta values were 10.4 & 10.1 K (L & R pols, respectively) over 7.6 - 9.0 GHz, where the Perley and Butler predicted flux is 5.1 Jy. An assumed gain value of 2.0 makes these scans consistent.

The second frequency window, over ∼8.6 - 10.0 GHz showed similar results to the first. However, the third frequency window, over ∼9.6 - 11.0 GHz showed similar results to scans 13/14 in the L pol. In the R pol (Fig.11 - middle), results were also ok below ∼10.7 GHz. However, above 10.7 GHz, the spectral response clearly showed RFI, which I suspect to be due to Starlink satellites (see Morgan et al. 2024). The suspected Starlink RFI is seen much more clearly in the R pol of the fourth frequency window - ∼10.6 - 12.0 GHz (Fig.11 - bottom). This was not seen in the L pol data, though there was a noticeable decrease in the

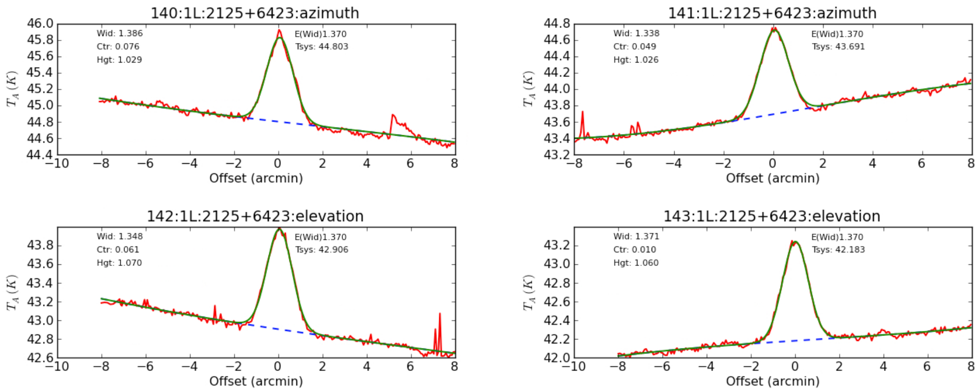

Figure 10: X-Band peak scans on 2125+6423

measured flux of 3C286, which went from 9.9 K at the low frequency end to ∼7.5 K at the high end. As noted in Morgan et al. (2024), 'chunks' of approximately 200 MHz are visible in the range 10.7 - 11.7 GHz, which correspond to *Starlink* satellite transmission channels. These are the presumed cause of the discontinuities in the bottom panel of Fig.11 and are explored more thoroughly in DePree et al. (2023).

The Perley-Butler flux of 3C286 at 12.0 GHz is 3.96 Jy so this is probably ok. Given the RFI - albeit highly polarised - it doesn't seem worthwhile to investigate much further at this point.

The TCal observations in Fig.11 were taken in wideband mode (all-pass filter), follow-up scans were taken in narrowband mode, where a 1.3 GHz filter is in place. This resulted in significantly lower flux values being measured (7.3 - 7.4 K). This is a noted feature of the X-band receiver (see below). RFI does seem to be present in these narrowband obs, based on the poor baselines but seems to have been considerably less impactful on these observations.

Scan 25 - Test tone injection: the response here was fine, there are symmetrical spikes seen at +/- 220 Hz which are $>$ 40 dB down compared to the test-tone spike. This is consistent with previous values.

Pulsar Observations:
XBand_VPM_Cal(Scans 26/27)/XBand_VPM_CalSearch(Scans 28/29)
Banks B, C & D failed to balance first time round (no scan taken). I put a second Balance command in script and the second time went fine. Results look ok to me, in that there is not a large 'roll-off' (see Fig.12). I have asked Ryan to double-check the results, his first impression was that the results were good but was going to have a closer look later.

Spike Investigation:
XBand_Spike_Check (Scans 30-33)
A known issue with the X-band receiver is the presence of spikes in the bandpass at certain, known frequencies. Walter is aware of these but was not able to take significant action this summer to address these. These most recent data continue to show the spikes, as seen in Fig.13 (red - data taken 17th Aug, 2024, white - this session).

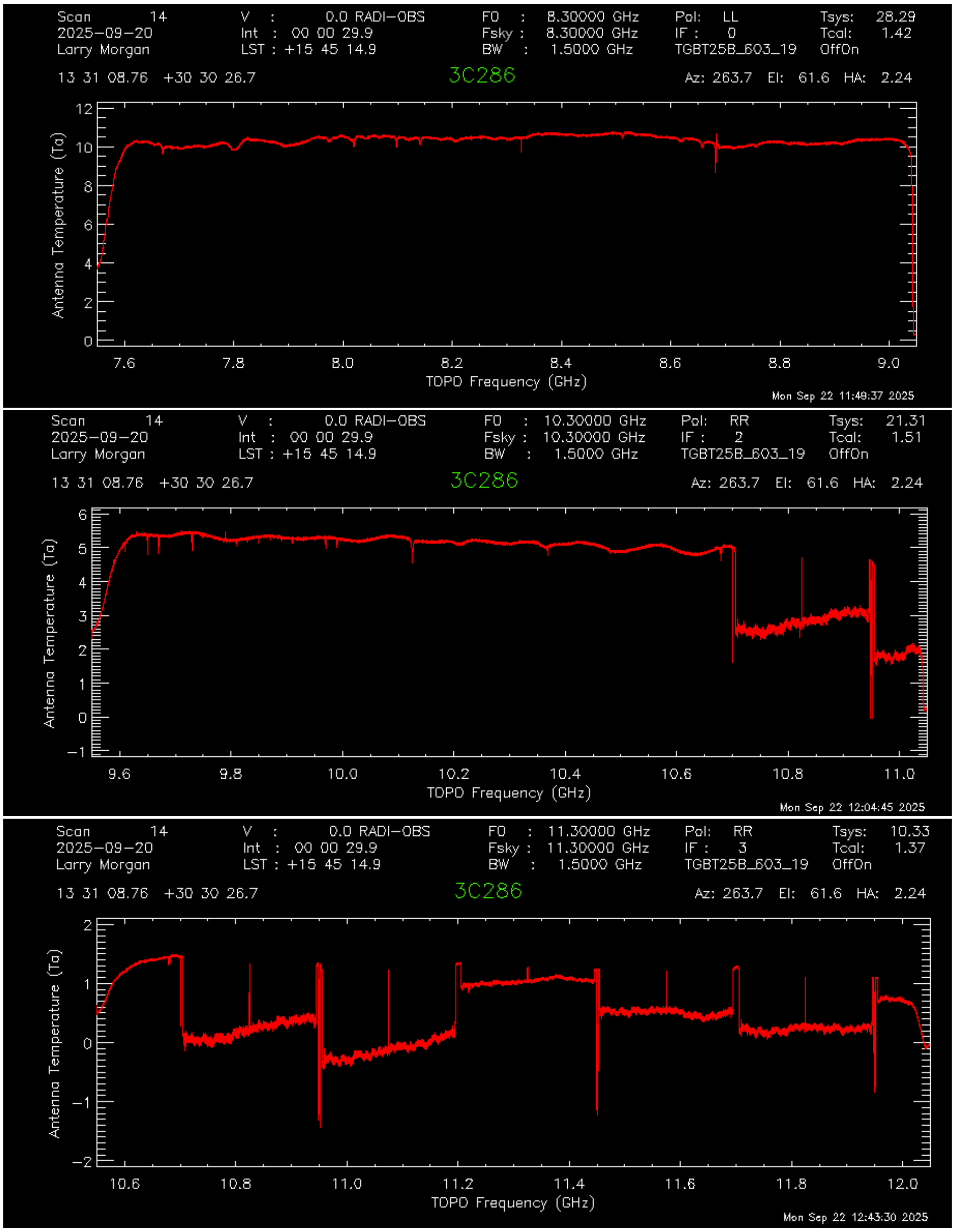

Figure 11: X-Band Flux Calibration scans on 3C286

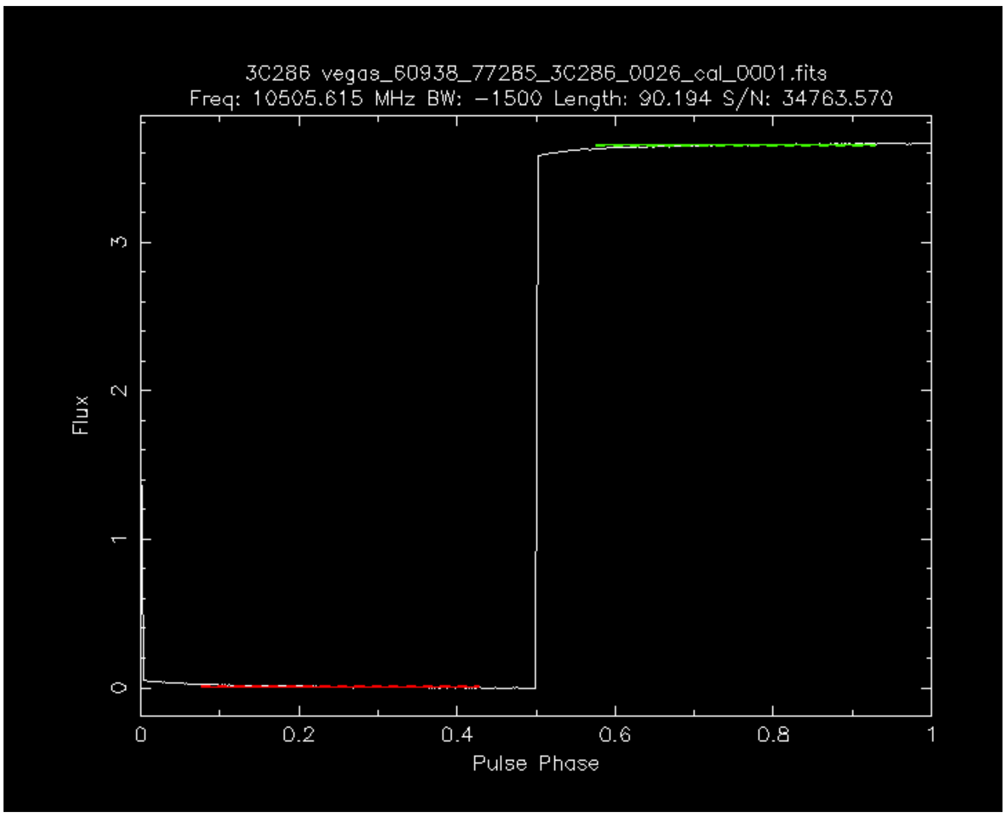

Figure 12: X-Band pulsar calibration scan on 3C286

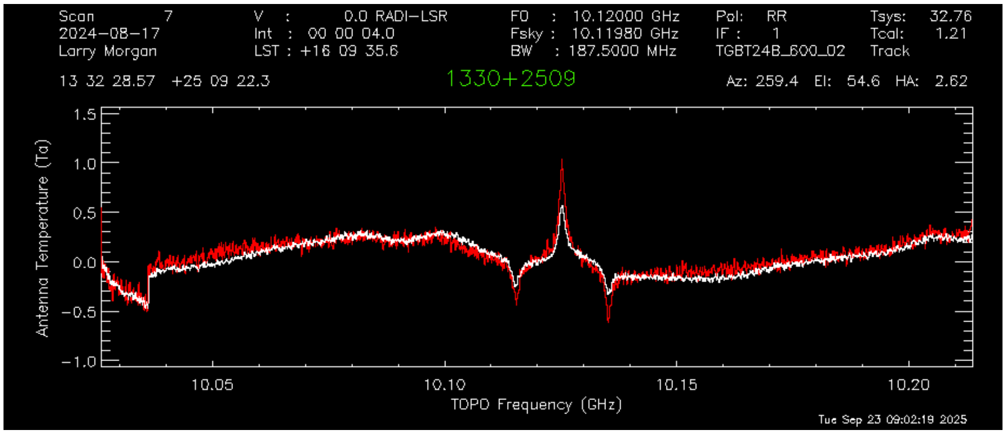

Figure 13: X-Band scan on 3C287 showing receiver 'spikes'

Spectral Line Observations:
XBand_Spec_FS/XBand_Spec_PS

I ran a series of spectral line observations, in both frequency- and position-switched modes on the sources DR21, SFO 34 and IC1396

- Tsys is considerably higher when observing DR21 (from ∼30 K to ∼60 K) - DR21 is a strong source, potentially strong enough to significantly alter power levels
- There are few immediately obvious spectral lines in the X-band frequency range, the better known are in TMC-1, which is currently below the horizon.
- Data are good, though no spectral line detection made. Without a confirmed source to compare to, there is little point integrating down to explore for lines.
- RMS is found to agree with sensitivity calculator, although only after careful baseline fitting and accounting for actual Tsys
- I see a big (3500 K) spike at 10.7 GHz in both pols. Some notes indicate that this may be due to the holography reference horn, although that was expected to be highly polarised. The operator and I made best efforts to turn off the holography horn and, as best as we can tell, this should be the case. It is possible that the switch is not functioning, Jason Ray will investigate. - Note added 16th April, 2026 - It has become evident that this spike is due to the holography test receiver, not the reference horn. Apparently the test horn cannot be turned off without someone physically pulling the AC plug.

Voyager I Observations:

Previous JPL backend observations of Voyager indicated SNR levels much lower than expected. As I had time to spare, I performed similar observations using VEGAS and could not replicate that result. I took spectra with multiple IF routings (all banks of VEGAS). From the JPL notes, the problematic routing was ODMs 6 & 8 through CMs 11 & 15. The default routing I initially used had CMs 11 & 15 going to bank G but through ODMs 5 & 7, I took a set of scans with that setup (scans 192/193) and found SNRs ranging from 34.9

- 35.8 (15.43 – 15.54 dB), where the bank G results were right in the middle at 35.47/15.55 dB. I also took a set of scans where I manually routed bank G to ODMs 6 & 8 through CMs 11 & 15 (scans 194/195). I had to manually balance the system but got good levels in VEGAS. In this case, the SNRs of the banks other than bank G gave SNRs from 39.2 to 41.1 (15.93 – 16.14 dB) while bank G had 36.3 / 15.60 dB.

My conclusion is that the JPL routing gives a slightly lower response to Voyager than others but nowhere near the deficit seen in the JPL obs (> 5 dB). In terms of the actual noise, the banks were all around the same. The values were a little higher than predicted by the sensitivity calculator but were pretty consistent from bank to bank. Note that banks E, F and H were not routed correctly due to my fiddling with the IF rack.

The Voyager I carrier signal was easily detected at $\sim$150 K. I made a quick map of the Voyager signal to check ephemeris positions (another suspected cause of the SNR deficit seen in the JPL observations). The signal was well-centred at the expected ephemeris position of 17:14:08.51 +12:12:51.9 (see Fig.14 - blue cross). These ephemeris were derived identically to the way they were in the JPL observations.

In summary, The large SNR deficit reported in the earlier JPL Voyager observations could not be reproduced with VEGAS. The specific IF routing used by JPL may introduce a small sensitivity loss, but only at the level of a few tenths of a dB, not the >5 dB discrepancy previously observed. The Voyager signal strength, system noise, and pointing/ephemeris all appeared nominal.

KFPA

- Ripple in initial peak/focus scans, resolved (or at least improved) after focus
- Ripple seen in general in APFs, worse for 3/7 than 4/6, this is consistent with previous results
- Scans 16 - 23, 29 - 36 & 42 - 54 showed considerable configuration/hardware issues (dropped packets errors). These were eventually resolved and other configurations used.
- Overall, scans showed considerably more RFI than expected from previous KFPA experience. Notably, severe, apparently new, RFI was consistently seen around 19.6 GHz (Fig.15) and 20.5 - 20.65 GHz. From communication with Sheldon Wasik, it is believed that this is due to Kuiper (Amazon's satellite broadband) downlinks. The VLA sees similar signals at the same frequency in their recent RFI scan, but didn't see it back in Spring. Kuiper has 500 MHz channels at:

  Ch1: 18700 – 19200 MHz, Ch2: 19200 – 19700 MHz, Ch3: 19700 - 20200 MHz

  This RFI was not present in all scans, notably it was not visible in the last scans of the session.
- Measured RMS values are $\sim$7% above theoretical. This could potentially be attributed to the RFI that was observed.

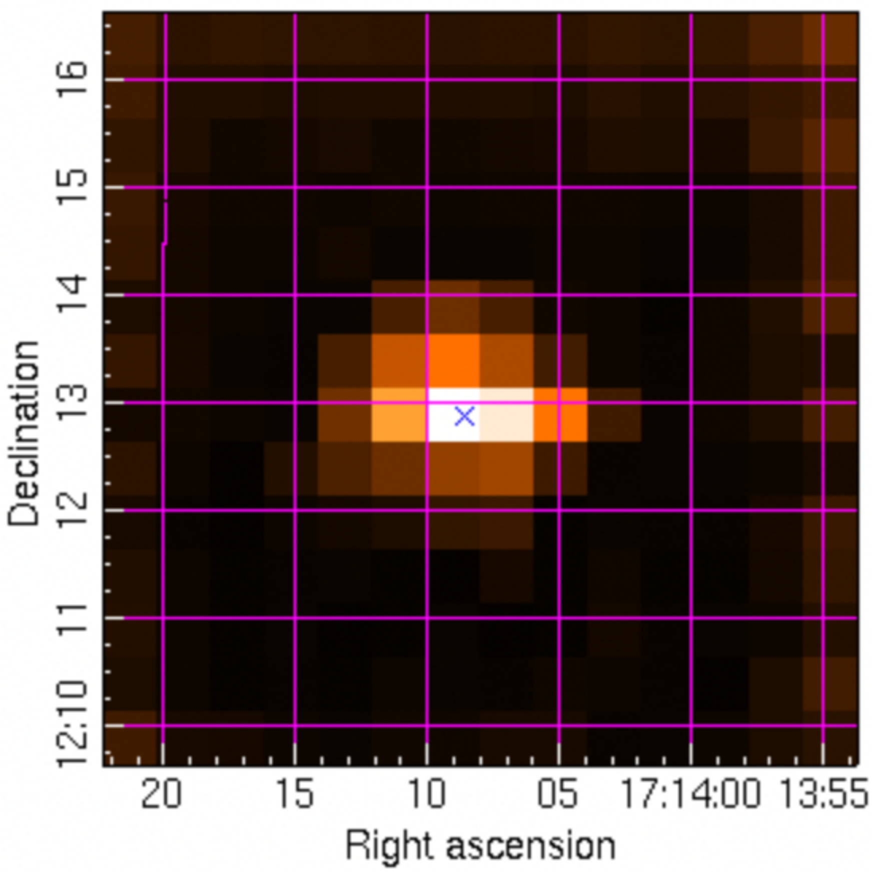

Figure 14: X-Band map of Voyager I at 8.420 GHz

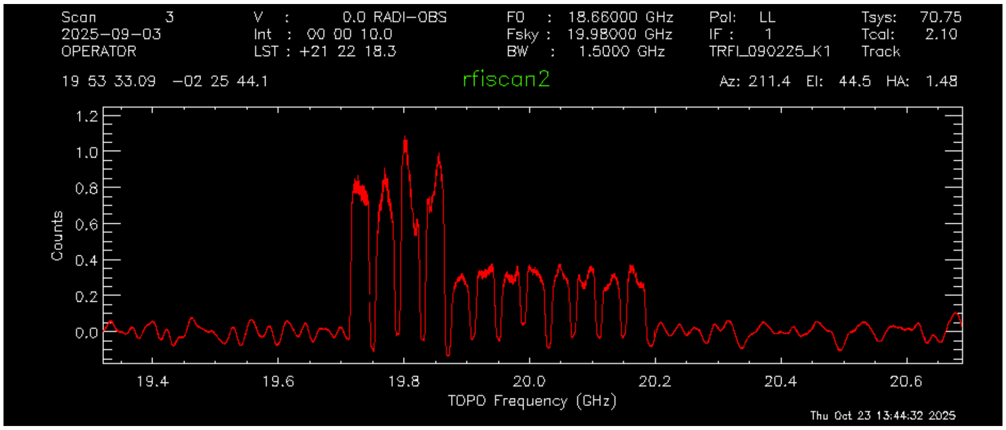

Figure 15: RFI seen with the KFPA at ∼19.7 - ∼20.2 GHz

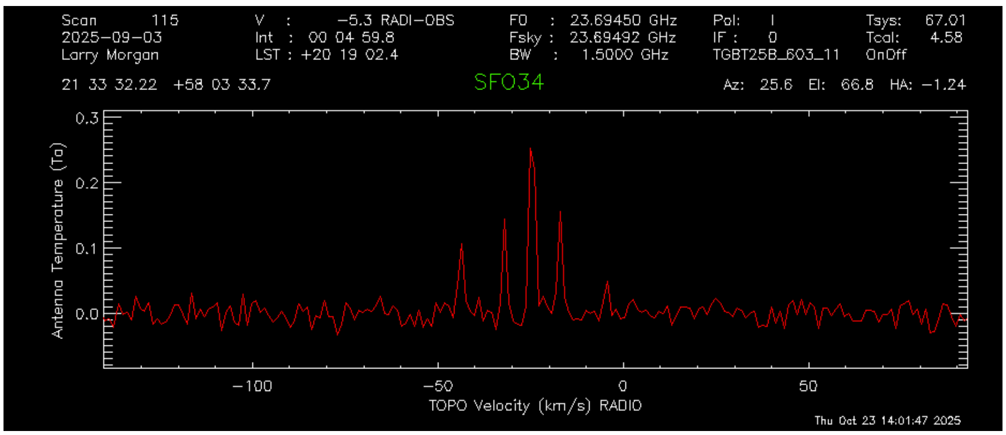

Figure 16: Ammonia (1,1) spectrum observed with the KFPA

- Tsys values range from 62 to 180 K and are noticeably higher for beams 5 - 7. This is broadly in keeping with pre-shutdown results and related (at least in part) to the TCals for these beams being less accurate.

- Spectral lines were visible towards known sources. As an example, the position-switched observation of scans 115/116 were a five-minute integration on a known ammonia source (SFO 34). Some visible baseline ripple was noted in the R pol of these data but this was within levels that could be accounted for with standard baseline fitting and removal (see Fig. 16).

- Due to lack of time the KFPA broadband mode was not explicitly tested during this session. Further tests on the 9th of September (TGBT25B_603_12) were run to investigate the stability of power levels in the KFPA, those tests indicate that the broadband mode was operating within normal parameters for both beams 1 and 2.

Appendix B:

Feed Defroster/Blower

A major focus of the MUSTANG2 recommissioning campaign was determining whether the new feed-defroster introduced excess vibration or detector noise. Dedicated tests were performed both with the receiver covered and during on-sky skydips and science observations. Power-spectrum analyses comparing blower-on and blower-off configurations (Fig.17) showed no statistically significant degradation in detector timestreams or noise properties attributable to the new blower, in contrast to older data obtained with the previous system. The instrument team concluded that the blower can remain on during MUSTANG-2 observations, while recommending periodic validation scans during future observing sessions.

Please note the following from the MUSTANG2 instrument team (including S. Dicker and C. Romero) regarding the feed defroster - 'blower':"

> As of now, the blower does not adversely affect MUSTANG-2 and we as the M2 instrument team give our blessing to leave the blower on during MUSTANG-2 observations. However, we are working on developing a data monitoring system to put in place to ensure that the blower continues to not affect MUSTANG-2 observations. And lastly, we recommend that during each MUSTANG-2 observing session observers take one set of science scans (4x 8 minute scans) with the blower off in order to have a comparison for each observing session.

Further details and analysis can be found at https://nrao.atlassian.net/wiki/x/BwA1Ew.

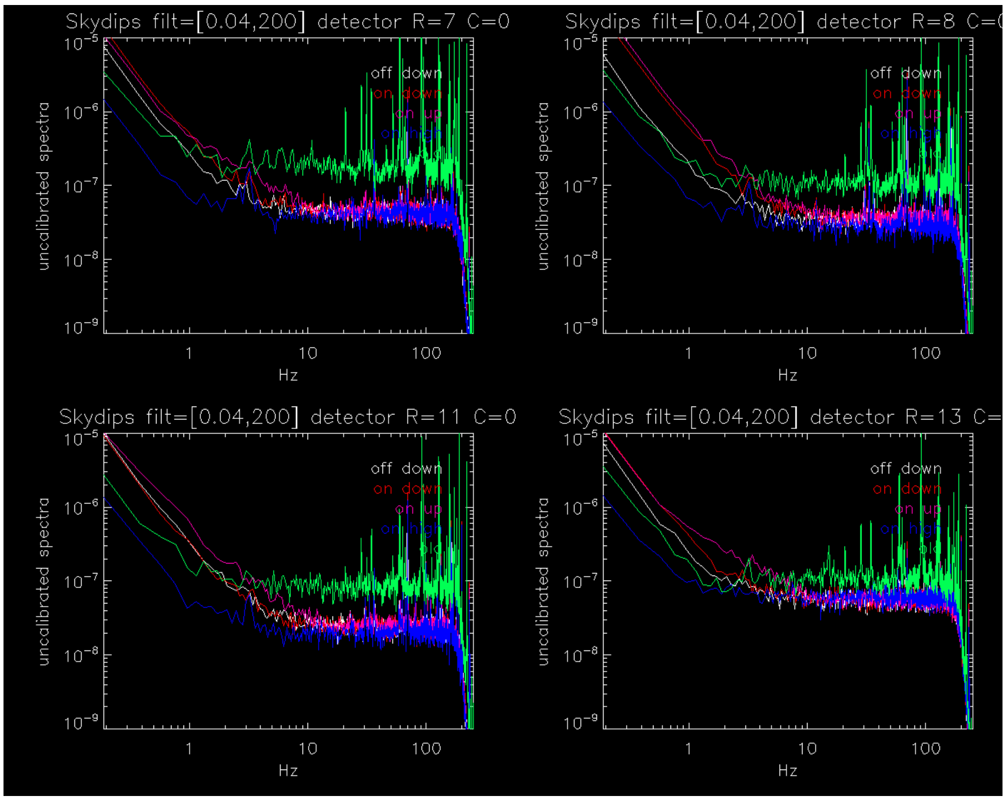

Figure 17: A comparison of the power spectra from 4 different detectors on Roach 1. The white and red spectra come from skydip scans which start at the top and go down in elevation, with the blower off and on, respectively. The pink spectra come from skydip scans starting at the bottom and going up in elevation, with the blower on. The blue spectra are a skydip done at high elevation with the blower on. The green spectra comes from a science scan (scan 1) from AGBT22B_242_02 with the blower on.